Hindawi
Advances in Civil Engineering
Volume 2018, Article ID 5304245, 14 pages
https://doi.org/10.1155/2018/5304245

Research Article

Seismic Vulnerability Assessment of Liquid Storage Tanks Isolated by Sliding-Based Systems

Alexandros Tsipianitis and Yiannis Tsompanakis

School of Environmental Engineering, Technical University of Crete, 73100 Chania, Greece

Correspondence should be addressed to Yiannis Tsompanakis; jt@science.tuc.gr

Received 28 February 2018; Revised 1 August 2018; Accepted 15 August 2018; Published 3 October 2018

Academic Editor: Tadeh Zirakian

Liquid-filled tanks are effective storage infrastructure for water, oil, and liquefied natural gas (LNG). Many such large-scale tanks are located in regions with high seismicity. Therefore, very frequently base isolation technology has to be adopted to reduce the dynamic distress of storage tanks, preventing the structure from typical modes of failure, such as elephant-foot buckling, diamond-shaped buckling, and roof damage caused by liquid sloshing. The cost-effective seismic design of base-isolated liquid storage tanks can be achieved by adopting performance-based design (PBD) principles. In this work, the focus is given on sliding-based systems, namely, single friction pendulum bearings (SFPBs), triple friction pendulum bearings (TFPBs), and mainly on the recently developed quintuple friction pendulum bearings (QFPBs). More specifically, the study is focused on the fragility analysis of tanks isolated by sliding-bearings, emphasizing on isolators' displacements due to near-fault earthquakes. In addition, a surrogate model has been developed for simulating the dynamic response of the superstructure (tank and liquid content) to achieve an optimal balance between computational efficiency and accuracy.

1. Introduction

The safe functioning of liquid storage tanks is of paramount importance, especially in seismic prone regions, since this severe natural hazard can lead to large-scale technological disasters, the so-called NATECH events. In general, cylindrical liquid storage tanks are structures that are widely used to store water, petrochemicals, and liquefied natural gas (LNG). Many such tanks are located in areas subjected to strong ground motions, and the seismic risk is higher compared to conventional structures due to devastating consequences. Failures of storage tanks due to earthquakes can cause leakages and explosions, as shown in many cases in the past earthquakes (Northridge (1994); Kobe (1995); Chi-Chi (1999)). In any case, a robust performance-based seismic design is required, as significant socioeconomical losses and environmental problems may result from even a minor failure.

Compared to ordinary structures (such as buildings and bridges), liquid storage tanks present different dynamic behavior due to liquid-tank interaction, since they are subjected to inertial earthquake loads and hydrodynamic pressures. The mechanical model of Housner [1] represents this behavior in a realistic manner. More specifically, the hydrodynamic response of the tank-liquid system is divided in two uncoupled components: the impulsive component (i.e., the lower part of the liquid that moves horizontally and follows the tank wall movements) and the convective component (i.e., the upper part of the liquid that generates the sloshing motion). Many studies [2–4] have shown the dominance of impulsive liquid component on the global tank seismic response. In contrast, the convective component can be neglected since it is associated to long periods (which is >6 sec for the examined tanks), that are substantially higher compared to the fundamental period of the tank-liquid system (approximately 2 sec for the examined isolated tanks, while it is <0.2 sec for fixed-base conditions). Thus, typical forms of storage tank failures in past earthquakes (e.g., "elephant foot" and "diamond shape" buckling types) are mostly related to the impulsive component and less caused by liquid sloshing [5].

Base-isolation technology is considered as an efficient approach to reduce the seismic vulnerability of liquid storage tanks. The fundamental concept of base-isolation is the "decoupling" of structure from ground motions by installing isolators, i.e., devices with low horizontal and high vertical stiffness to accommodate the vertical loads of the structure. Therefore, the stresses and accelerations imposed on the tank are notably reduced, even if the displacements are quite high due to the increased deformability of the flexible bearings [6, 7]. Some large-scale liquid storage tanks isolated by friction isolators are presented in EPS [8]. Firstly, two LNG tanks of Revithoussa, Greece, each having a capacity of 65.000 m^3, are equipped with totally 424 SFPB isolators. Secondly, two large LNG tanks located in Melchorita facility in Peru [9] are isolated by TFPBs, where earthquakes with magnitude >8 of Richter scale may occur.

Many studies have been devoted to the seismic analysis and vulnerability assessment of liquid storage tanks base-isolated with friction isolators. Firstly, Wang et al. [10] studied the effectiveness of SFPBs installed at the base of cylindrical tanks using a hybrid structure-hydrodynamic numerical model. Parameters such as tank aspect ratio, friction coefficient of SFPBs and earthquake intensity were examined. It was concluded that the impulsive pressures can be significantly reduced due to seismic isolation, while the convective pressures were slightly changed. Jadhav and Jangid [11] compared the seismic response of liquid storage tanks isolated by elastomeric bearings and sliding systems, while the continuous liquid mass of the tank was modeled as lumped masses, namely, sloshing mass, impulsive mass, and rigid mass. Using a similar simplified model of the masses, Panchal and Jangid [12] investigated the seismic response of liquid storage tanks isolated with variable friction pendulum system (VFPS). Based on the assumption of the concentrated masses, the kinematic equations for the VFPS and the storage tank were formed and solved. It was concluded that using VFPS as base-isolation system for liquid storage tanks, their seismic response could be controlled within desirable limits.

The work of Abali and Uckan [13] reported the efficiency of SFPBs in controlling the earthquake response of slender tanks compared to squat tanks. More specifically, a parametric analysis was conducted taking into account isolation period, tank aspect ratio and coefficient of friction. It was derived that base shear was reduced for both squat and slender tanks. Conversely, sloshing displacements of squat tanks were not significantly changed. The double variable frequency pendulum system (DVFPS) that isolated the liquid storage tank was included in the numerical model of Soni et al. [14]. The examined DVFPS was analyzed for different geometry and friction coefficient values. The main conclusions derived from this study were that DVFPS with higher initial stiffness from top sliding surface to bottom presented better behavior for slender tank, while the isolator having the same initial stiffness and coefficient of friction performed better for the squat tank.

Seleemah and El-Sharkawy [15] investigated the dynamic response of elevated squat and slender liquid storage tanks isolated by elastomeric and sliding bearings (SFPB). In addition, the behavior of the storage tanks was compared for the cases where the isolators were placed at the bottom or at the top of the supporting structure. It was reported that base isolation affected in a beneficial manner the slender tanks and less the corresponding squat tanks. Furthermore, when an elevated tank was isolated with SFPBs, it presented better seismic performance than with elastomeric bearings. In addition, the examined tank presented better seismic behavior when isolators were placed at the top of the shaft support.

Panchal and Jangid [16] examined the seismic behavior of liquid storage tanks equipped with variable curvature friction pendulum system (VCFPS) under near-fault ground motions. The most important parameters for this investigation were the fundamental period, the friction coefficient, and the tank aspect ratio. It was found that the VCFPS is a quite effective seismic isolation device in controlling base shear, sloshing displacement, and the impulsive displacement of liquid storage tanks.

Moeindarbari et al. [17] investigated the efficiency of SFPB and TFPB installed at elevated liquid storage tanks subjected to multihazard level excitations. TFPB is capable of performing multiple level analysis at different hazard scenarios, such as Service Level Earthquake (SLE), Design Basis Earthquake (DBE), and Maximum Credible Earthquake (MCE). Hence, the results revealed that TFPB outperformed the SFPB, since the adaptive performance of TFPB played an important role in decreasing the seismic demand on the liquid storage tanks. Similarly, the effectiveness of two isolation systems of elevated storage tanks was studied by Paolacci [18]. Records from the Kocaeli Earthquake (1999) were used for the dynamic analysis of high damping rubber bearing (HDRB) and SFPB installed at the elevated tanks located in Habas pharmaceutics plant in Turkey. It was concluded that elevated tanks isolated both by HDRB and SFPB presented major reductions in base shear as well as stress levels in the tank's wall. Due to the limitation of maximum bearing displacement and the higher value of sloshing displacement for the HDRB, the SFPB was considered as the superior isolation scheme for this specific case study.

Bagheri and Farajian [19] investigated the impact of PGA level and special characteristics of near-fault impulses on the earthquake performance of liquid storage tanks isolated by SFPBs. A mechanical model that accurately estimated the seismic response of the liquid storage tank was adopted. The results indicated that SFPB is an effective isolation system, capable of reducing critical parameters, such as impulsive displacement, overturning moment, and base shear, while the sloshing displacement did not present significant changes. Phan et al. [20] conducted a seismic fragility analysis of elevated liquid storage tanks isolated by concave sliding bearings (CSB). For this purpose, a lumped-mass simplified model was used for the examined tank. The cloud method was applied for the seismic fragility assessment, where nonlinear dynamic analysis through a linear regression-based probabilistic model was implemented. CSB scheme was found to be an effective isolation system for the reduction of the seismic demand on the tank.

In the majority of the aforementioned studies, the seismic response and/or vulnerability assessment of liquid storage tanks base-isolated by SFPBs or TFPBs was investigated. The influence of many critical parameters (i.e., base shear, aspect ratio, isolation period, etc.) on the results was examined, and it was proven that single-stage (SFPBs) and multistage (such as TFPBs) friction bearings were effective in reducing the seismic response, even when strong near-fault excitations were imposed. On the other hand, the newly appeared QFPB is a state-of-the-art seismic isolation device capable of accommodating very large displacements and performing complex multistage behavior [21]. It consists of six spherical sliding surfaces with five effective pendula. To the best of the authors' knowledge, seismic vulnerability assessment of liquid storage tanks isolated by QFPBs has not been reported in the literature.

Accordingly, in this study, which is an extension of a recent conference paper of the authors [22], the seismic vulnerability assessment of liquid-filled tanks isolated by different types of friction isolators is examined, following performance-based design (PBD) principles. More specifically, the study is focused on the response of single-surface isolators SFPBs, and the corresponding multiple-surface isolators: TFPBs and QFPBs. Utilizing peak ground acceleration (PGA) as the intensity measure (IM) and isolator displacement as the damage index (DI) for three earthquake hazard levels, fragility analysis is performed for each of these three sliding bearing configurations. Surrogate numerical models, based on the work of Bakalis et al. [23], have been developed for modeling both squat and slender liquid storage tanks. Compared to detailed finite element simulations, such models combine the minimization of computational cost with adequate accuracy of the dynamic response calculations. They consist of a concentrated impulsive mass that is attached to a vertical beam element supported by rigid beam spokes. Moreover, they can be implemented utilizing any general-purpose structural analysis software and can be used for either static or dynamic analysis.

2. Friction-Based Isolation Devices

2.1. Single Friction Pendulum Bearings. Figure 1(a) depicts a typical SFPB, which is a device that uses its special geometrical setting to provide seismic isolation [24]. The pendulum motion is represented by the spherical bearing surface, while the period of the isolator depends on the radius of curvature of the concave sliding surface. Additionally, another critical feature of SFPB is that the center of resistance coincides with the center of mass. Thus, the torsion response of the superstructure is limited. Therefore, parameters such as structural response, ductility, and energy dissipation can be controlled, and damage to building structural and nonstructural members and contents can be minimized or even avoided.

2.2. Triple Friction Pendulum Bearings. TFPB is an adaptive sliding isolation system that can exhibit different stiffness and damping properties during its operation [25] and represents the new generation of friction isolators. It utilizes multiple spherical concave sliding surfaces, thus, both low transmissibility of vibration to the superstructure and zero residual displacements at the sliding structure after an earthquake are provided [26]. Hence, its operation is different from the conventional sliding bearings that exhibit constant stiffness and energy dissipation. In TFPBs, different combinations of curvature and friction of sliding interfaces can be selected. Moreover, these parameters can be adjusted depending on the imposed excitation levels. Therefore, multiple performance objectives can be achieved, which is ideal from a PBD perspective.

A TFPB consists of three friction pendulum mechanisms, which are activated at different stages as the seismic demand is amplified. As illustrated in Figure 1(b), these mechanisms are created via four concave surfaces in a single bearing. According to Constantinou et al. [27], the two inner surfaces share the same values for their friction coefficients ($\mu_2 = \mu_3$) and radius of curvature ($R_2 = R_3$). Analogously, it is also common that the outer concave surfaces have the same values ($\mu_1 = \mu_4$) and ($R_1 = R_4$). In a typical TFPB functioning, sliding occurs in different surfaces as the displacement demand increases. When TFPB approaches its maximum displacement capacity, the surfaces change again due to the fact that the displacement restraints of the sliders are reached, causing incremental hardening behavior [28].

The calculated values of the force-displacement curve for the TFPB configuration that has been used in the current investigation are shown in Figure 2(a). As it can be easily noticed, it is divided into several parts, depending on the selection of geometrical and frictional parameters. The horizontal force of TFPB is a combination of the friction force and the restoring force due to the curvature of the spherical surfaces. Normalized horizontal force, F/W, is conveniently used, since the resultant force, F, is proportional to the vertical force, W. Evidently, TFPB is ideal for PBD, since by selecting appropriate values for friction coefficients and radii of curvature for each surface, different behavior under service level earthquake (SLE), where sliding occurs on surfaces 2 and 3; design basis earthquake (DBE), where motion stops on surface 2 and sliding occurs on surfaces 1 and 3; and maximum considered earthquake (MCE), where sliding occurs on surfaces 1 and 4 can be achieved [8, 17].

2.3. Quintuple Friction Pendulum Bearings. According to Lee and Constantinou [21], the newly developed QFPB is an extended version of TFPB. In particular, it consists of six spherical sliding surfaces, five effective pendula, and nine operation regimes (Figure 1(c)) in a single bearing. The computed force-displacement curve of the examined QFPB is depicted in Figure 2(b). The adaptability of isolator behavior is increased due to the increased number of pendula and sliding patterns. Thus, although the functioning is similar, it is capable of a more complex and multistage performance compared to TFPB. Additionally, QFPB is ideal for high displacement demands due to severe earthquake excitations.

Similar to TFPBs, QFPBs can also be implemented within a PBD framework. Although the number of sliding

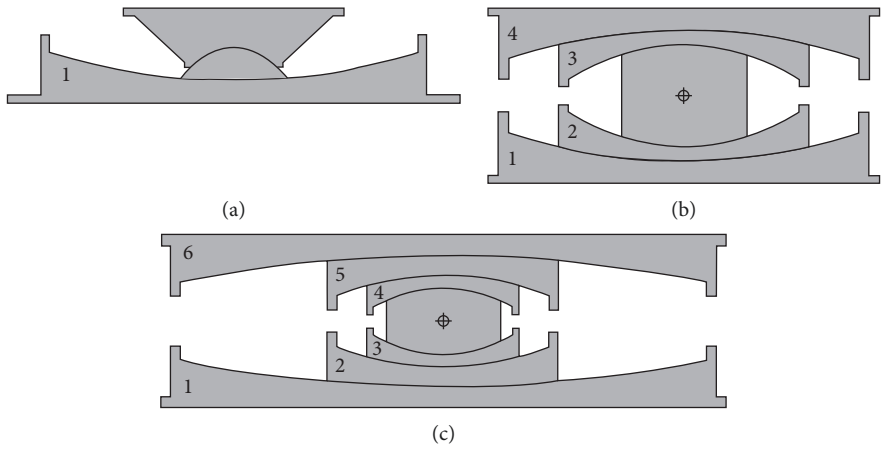

Figure 1: (a) Section view of SFPBs, (b) TFPBs, and (c) QFPBs, where numbers correspond to different sliding surfaces (adopted from [21]).

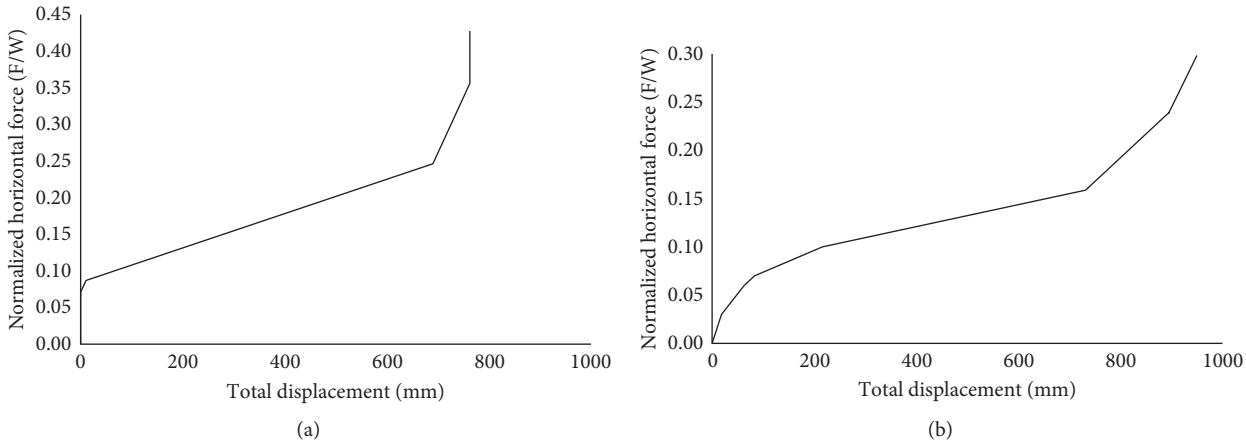

Figure 2: (a) Computed force-displacement curves for the examined bearing configurations: (a) TFPBs and (b) QFPBs.

surfaces is increased (six for QFPBs vs. four in the case of TFPBs as shown in Figures 2(a) and 2(b), respectively), the performance levels remain the same in this investigation, in particular, service level earthquake (SLE), where sliding occurs on surfaces 3 and 4; design basis earthquake (DBE), where motion stops on surface 6 and sliding occurs on surfaces 2 and 5; and maximum considered earthquake (MCE), where sliding occurs on surface 1.

2.3.1. Model Validation. In this section, the analytical and experimental validation of QFPBs utilizing finite element software SAP2000 [29] is presented, following the recommendations of Lee and Constantinou [21]. The isolator is simulated in the software as a series model, combining one triple friction pendulum (FP) element with one double FP element. The double FP isolator is actually a "condensed" triple FP element. This is achieved by specifying arbitrary values of the radius of curvature and friction coefficient that lead to motion initiation of the inner sliding surfaces. In this manner, the double FP isolator operation is performed utilizing SAP2000 (Figure 3(a)). The configuration examined has friction coefficient values: $\mu_3 = \mu_4 < \mu_5 \leq \mu_2 < \mu_6 \leq \mu_1$.

Figures 4 and 5, respectively, illustrate the force-displacement curves taken from a recent study [21] for the experimental (tested in the experimental setup at the University at Buffalo [30]) and the analytical QFPB models, which are compared to the numerical results of the same configurations obtained herein utilizing SAP2000 software. Firstly, the experimental model of one QFPB (Table 1) based on the multistage experimental setup of the isolator tested at the University at Buffalo [30] is validated numerically via SAP2000 software. A harmonic excitation with frequency equal to 0.005 Hz was imposed to the tested QFPB, together with a constant vertical load of $W = 88964.4$ N. The displacement amplitude of the imposed harmonic motion was equal to 127 mm, since this was the displacement capacity of the testing device. Figure 4 illustrates the validation of QFPB with respect to the experimental model. As it can be noticed in this plot, there is an excellent matching of the force-displacement curves of the experimental model and the corresponding isolator model developed in SAP2000.

The second validation is performed by comparing the obtained numerical results with the corresponding ones of the analytical QFPB model for another case study [21]. In this example, a sinusoidal harmonic excitation is imposed to

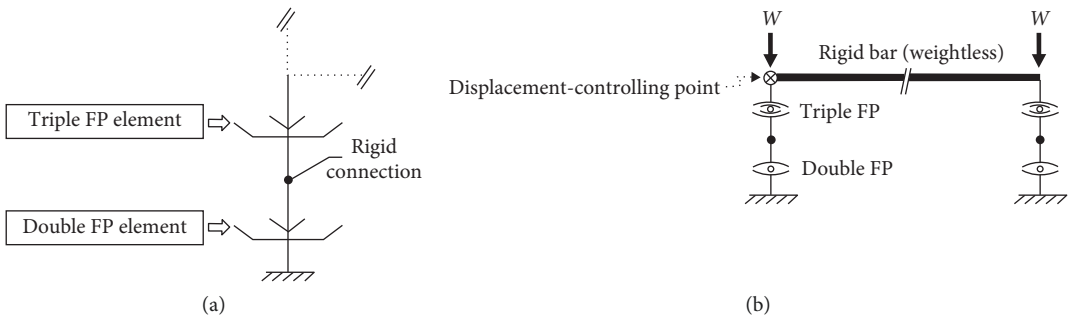

Figure 3: (a) Series model of QFPB with a pair of double and triple FP elements and (b) model equipped with QFPBs as implemented in SAP2000 (adopted from [21]).

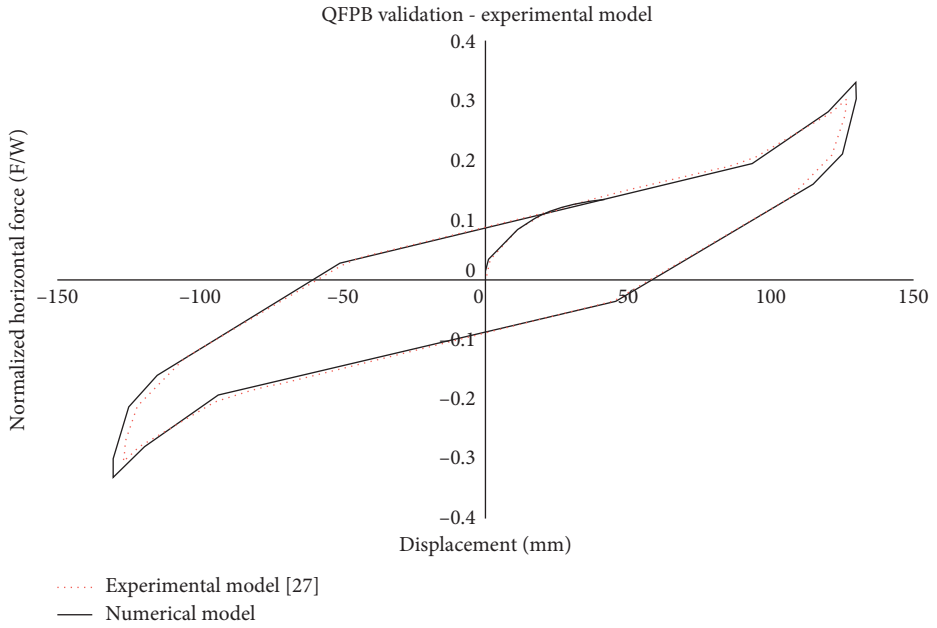

Figure 4: Comparison of current numerical QFPB model with experimental results derived from Lee and Constantinou [21].

the isolator, having an amplitude of approximately 1 m, equal to the displacement limit of the analytical model. Further information considering the force-displacement expressions used for the current validation can be found in the detailed study of [21]. By observing Figure 5, it can be noticed that the numerical isolator model developed utilizing SAP2000 captures exactly the behavior of the analytical model. Hence, the QFPB configuration presented in Figure 5 has been considered suitable for the fragility analysis of the examined liquid storage tanks. Consequently, after the successful validation of the present numerical implementation of the examined isolators, a detailed parametric study has been performed regarding their implementation for the seismic isolation of liquid storage tanks, as it will be presented in the sequence.

3. Multistep Dynamic Analysis

For such critical infrastructures as liquid storage tanks, a wide range of ground motion records should be taken into account for the reliable implementation of performance-based design. Consequently, a huge number of nonlinear dynamic analyses need to be executed in an incremental manner. Incremental dynamic analysis (IDA) and multiple-stripe dynamic analysis (MSDA) are the most frequently applied methods [31]. Such methods are widely used in earthquake engineering for seismic performance assessment of various types of structures. They are based on the simple concept of scaling each ground motion until it leads to the collapse of the examined structure. MSDA is ideal for performance-based evaluation of structures using a set of ground motion records at multiple performance levels. Many sets of analyses are performed for multiple peak ground acceleration (PGA) levels, where at each analysis (stripe) a number of structural analyses are performed for a group of ground motion records, which are scaled every time to a specific PGA value. In this way, a set of intensity measure and damage index values is produced.

Therefore, obtaining the relation between the seismic intensity level and the corresponding maximum response quantity of the base isolation system is the main objective of these multistep procedures. A suitable intensity measure (IM) and an engineering demand parameter (EDP) describe

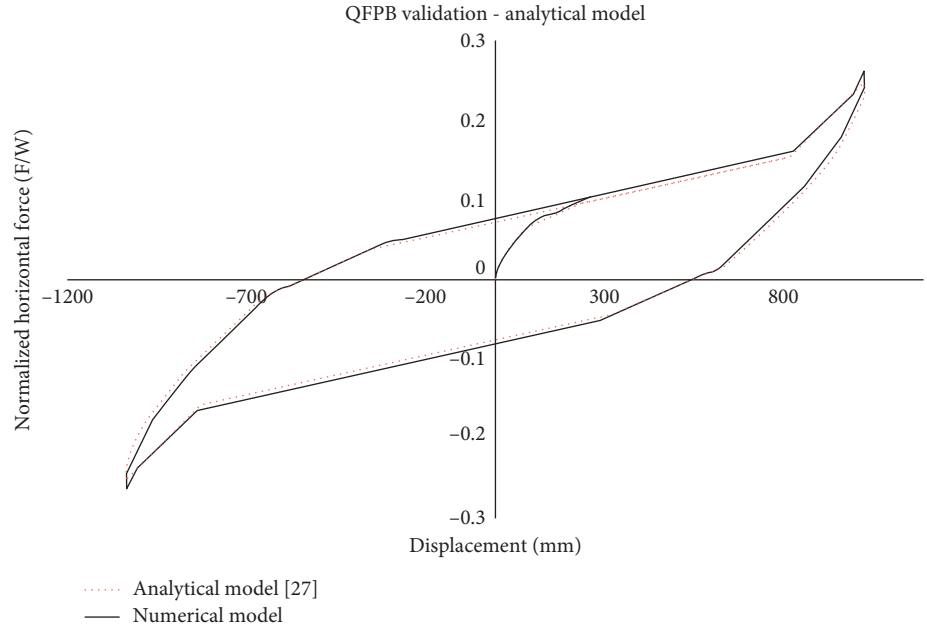

Figure 5: Comparison of current numerical QFPB model with analytical results derived from Lee and Constantinou [21].

Table 1: Parameters of the QFPB model (taken from [21]).

Radius (m)	Height (m)	Coefficient of friction	Displacement capacity (m)
$R_1 = 0.4572$	$h_1 = 0.03556$	$\mu_1 = 0.12$	$d_1 = 0.0381$
$R_2 = 0.2032$	$h_2 = 0.03048$	$\mu_2 = 0.085$	$d_2 = 0.03302$
$R_3 = 0.0508$	$h_3 = 0.02286$	$\mu_3 = 0.015$	$d_3 = 0.01397$
$R_4 = 0.0508$	$h_4 = 0.02286$	$\mu_4 = 0.015$	$d_4 = 0.01397$
$R_5 = 0.2032$	$h_5 = 0.03048$	$\mu_5 = 0.035$	$d_5 = 0.03302$
$R_6 = 0.4572$	$h_6 = 0.03556$	$\mu_6 = 0.11$	$d_6 = 0.0381$

the seismic intensity level and the friction isolators response, respectively. Generally, the following steps are implemented for both MSDA and IDA procedures: (a) create an efficient nonlinear finite element model for performing repeated nonlinear dynamic analyses, (b) select an appropriate group of natural or artificial accelerograms, (c) choose proper IM and EDP, and (d) select scaling factors in order to run the analyses and obtain the IM-EDP curves.

4. Fragility Function Evaluation

Seismic fragility is associated to the probability of exceedance of a limit state for a given seismic intensity level. Typically, a fragility function is defined by a lognormal cumulative distribution function (CDF) [32]:

$$P(C|IM = x) = \Phi\left(\frac{\ln(x/\theta)}{\beta}\right), \tag{1}$$

where $P(C|IM = x)$ is the probability that a ground motion with $IM = x$ will lead to structural collapse, Φ denotes the standard normal CDF, θ is the median of the fragility function and β is the standard deviation of $\ln\theta$. Regarding the selection of IM, the PGA is a valid choice for liquid storage tanks due to the impulsive load pattern [20, 33, 34].

In the current study, fragility curves related to SFPBs, TFPBs, and QFPBs displacements are calculated for different performance levels, namely, 50% probability of exceedance in 50 years (i.e., SLE), 10% probability of exceedance in 50 years (i.e., DBE), and 2% probability of exceedance in 50 years (i.e., MCE). In the present investigation, the methodology for fragility function fitting proposed by Baker [32] has been adopted, in which by performing repeated dynamic analyses for all ground motions and for each IM level a number of failures (i.e., in terms of isolators' displacement) is determined. The probability of z_j failures being observed out of n_j ground motions having $IM = x_j$ is represented by the following binomial distribution [32]:

$$P\left(z_j \text{ collapses in } n_j \text{ ground motions}\right) = \binom{n_j}{z_j} p_j^{z_j} \cdot \left(1 - p_j\right)^{n_j - z_j}, \tag{2}$$

in which p_j is the probability that a ground motion with $IM = x_j$ will cause failure of the structure.

When analysis data are obtained at multiple IM levels, the product of the binomial probabilities at each level provides the likelihood for the entire data set:

$$\text{likelihood} = \prod_{j=1}^{m} \binom{n_j}{z_j} p_j^{z_j} \left(1 - p_j\right)^{n_j - z_j}, \tag{3}$$

where m is the number of IM levels and Π is a product over all levels. Substituting Equation (1) for p_j, the fragility parameters are explicitly included in the likelihood function:

$$\text{likelihood} = \prod_{j=1}^{m} \binom{n_j}{z_j} \Phi\left(\frac{\ln(x_j/\theta)}{\beta}\right)^{z_j} \cdot \left(1 - \Phi\left(\frac{\ln(x_j/\theta)}{\beta}\right)\right)^{n_j - z_j}. \quad (4)$$

While the maximization of the likelihood function produces the estimates of the fragility function parameters as follows:

$$\{\hat{\theta}, \hat{\beta}\} = \arg_{\theta,\beta} \max \sum_{j=1}^{m} \left\{ \ln \binom{n_j}{z_j} + z_j \ln \Phi\left(\frac{\ln(x_j/\theta)}{\beta}\right) + (n_j - z_j) \ln \Phi\left(\frac{\ln(x_j/\theta)}{\beta}\right) \right\}. \quad (5)$$

5. Base-Isolated Liquid Storage Tanks

5.1. General Details. The storage tank models presented by Haroun [35] (Tank B and T types) are used in this work. More specifically, Tank B (Figure 6(a)) is a squat cylindrical tank with height to radius ratio $H/R = 0.67$. The radius of the first tank is $R = 18.29$ m, the height of liquid surface is $H = 12.192$ m, the tank wall thickness is $t = 0.0254$ m, and the total weight of the liquid content is $W = 126273.45$ kN. The second model (Figure 6(b)) is a slender cylindrical tank with height to radius ratio $H/R = 3$. Tank T has radius $R = 7.32$ m, height $H = 21.96$ m, width $t = 0.0254$ m, and the liquid weight is $W = 36245.4$ kN. The fundamental periods of the two tank-liquid systems are $T_{f\text{-}B} = 0.162$ sec and $T_{f\text{-}T} = 0.188$ sec, for Tanks B and T, respectively.

5.2. Surrogate Models. Modeling of liquid storage tanks is not an easy task due to the hydrodynamic response of the tank-liquid system [13, 19, 23]. In general, detailed finite-element models are computationally demanding [36]. To reduce the computational load and model complexity, one common approach is to develop valid simplified models to effectively replace the complicated three-dimensional (3D) models [37]. Therefore, a simplified representation of the liquid storage tank is adopted herein, based on the so-called "Joystick model" of fixed-base tanks [23]. The developed Joystick model consists of a vertical beam element carrying the impulsive mass that is supported by fully rigid beam-spokes, which in turn are supported by the sliding bearings (Figure 6). The two examined models are validated by accurate matching of the impulsive fundamental period (T_i) provided by Eurocode 8-Part 4 [38] recommendations for liquid storage tanks.

As aforementioned, the hydrodynamic response is mainly affected by the impulsive liquid component. The convective liquid mass is neglected since several studies [18, 39, 40] have proven that although the impulsive pressure is reduced due to seismic isolation, the convective pressure remains practically unchanged. Moreover, the effects of the convective part of liquid content can be separately estimated [23]. In the developed surrogate model, the weight of the water is represented as lumped masses at the base beam-spokes of the tank (Figure 6). Therefore, the vertical load is directly applied to the friction isolation devices. The self-weight of the tank can be omitted as it is only 5% of the total tank mass [12, 16, 29, 34].

5.3. Design of Isolation Bearings. Generally, the design of structural isolation systems is an iterative process, since the bearing properties are influenced by the structural properties. Firstly, the maximum bearing displacement has to be evaluated, which is mostly affected by the target period of the isolated system, the weight of the superstructure, and the intensity level of the imposed seismic excitation.

In this study, the equivalent linear force (ELF) procedure according to Eurocode 8 (Soil A, $\gamma_i = 1.4$, $a_g = 0.36$ g) is applied for the preliminary design of tank isolation system [41]. The selected SFPB has friction coefficient $\mu = 0.08$, radius of curvature $R = 1.88$ m, theoretical period of 2.75 sec, and displacement limit of 0.305 m. The TFPB properties are listed in Table 2 and the total displacement limit for MCE level is 0.762 m, which is the sum of all partial displacement limits. Finally, a QFPB with the properties is shown in Table 3, while the total displacement limit of 1.04 m (i.e., the sum of all displacements in Table 3) for MCE level is computed following the methodology developed by Lee and Constantinou [21]. The vertical load on the bearings is equal to 2.9 MN for the squat tank and 2.7 MN for the slender tank, respectively.

5.4. Numerical Modeling and Earthquake Selection. As previously mentioned, each Joystick tank model, which is supported either on SFPBs, TFPBs, or QFPBs, is simulated utilizing the finite element software SAP2000 [29]. This simplified tank model consists of a vertical beam element carrying the impulsive mass and is supported by fully rigid beam-spokes that represent the tank base. The properties of the vertical beam were determined using simple structural analysis calculations following the recommendations of Eurocode 8-Part 4 [38]. In order to test the isolators under strong excitations, the near-fault earthquake ground motion set produced within the FEMA/SAC Project [42] is used in this investigation (www.nisee.berkeley.edu/elibrary/files/documents/data/strong_motion/sacsteel/motions/nearfault.htm). Time-histories derived from natural and simulated records are included in this suite of accelerograms. The use of a sufficient number of properly selected excitations (i.e., exhibiting certain characteristics to avoid using an excessive number of records and maintaining an optimal balance among computational cost and accuracy) in conjunction with a huge number of MSDA/IDA analyses is imperative in order to achieve reliable fragility analysis results. The specific suite of acceleration time-histories consists such a case, since it is a well-established set of impulsive ground motions, with epicentral distances less than 10 km and very high PGA recorded values ranging from 0.45 g to 1.07 g, which is usually used in fragility analysis studies [43].

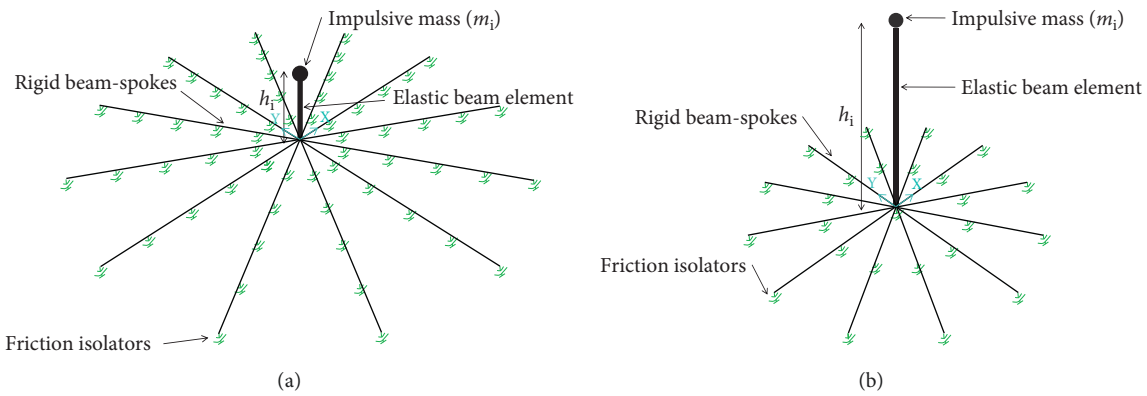

Figure 6: Joystick models for a squat (a) and a slender tank (b).

Table 2: Design parameters for the TFPB isolated squat tank.

Friction coefficient	Radii of curvature (m)	Height (m)	Effective radii (m)	Displacement limit (m)
$\mu_{1,\text{slow}} = \mu_{4,\text{slow}} = 0.09$	$R_1 = R_4 = 2.235$	$h_1 = h_4 = 0.102$	$R_{1,\text{eff}} = R_{4,\text{eff}} = 2.133$	$d_1^* = d_4^* = 0.34$
$\mu_{2,\text{slow}} = \mu_{3,\text{slow}} = 0.071$	$R_2 = R_3 = 0.406$	$h_2 = h_3 = 0.076$	$R_{2,\text{eff}} = R_{3,\text{eff}} = 0.33$	$d_2^* = d_3^* = 0.041$

Table 3: Design parameters for the QFPB isolated squat tank.

Sliding surface	Effective radius of curvature (m)	Coefficient of friction	Displacement limit (m)
Surface 1	$R_{1,\text{eff}} = 5.84$	$\mu_1 = 0.1$	$d_1^* = 0.344$
Surface 2	$R_{2,\text{eff}} = 1.12$	$\mu_2 = 0.06$	$d_2^* = 0.134$
Surface 3	$R_{3,\text{eff}} = 0.508$	$\mu_3 = 0.01$	$d_3^* = 0.047$
Surface 4	$R_{4,\text{eff}} = 0.508$	$\mu_4 = 0.01$	$d_4^* = 0.047$
Surface 5	$R_{5,\text{eff}} = 1.12$	$\mu_5 = 0.03$	$d_5^* = 0.134$
Surface 6	$R_{6,\text{eff}} = 3.76$	$\mu_6 = 0.07$	$d_6^* = 0.337$

More specifically, for each of the three performance levels, the selected twenty earthquake records are suitably scaled and then they are imposed at the isolated Joystick models until displacement limits are reached. Regarding the numerical analyses, the fast nonlinear analysis (FNA) is ideal for structural systems in which the nonlinear response is concentrated at the base isolation system, while the superstructure remains elastic [29]. FNA is a computationally efficient approach and is often preferred than direct-integration schemes. The damping for the structural system is taken equal to 5% and for the impulsive liquid component equal to 2% [44, 45].

6. Numerical Results

6.1. Fragility Curves. As aforementioned, maximum displacement of the different TFPBs and QFPBs sliding schemes is associated to three hazard levels. Accordingly, using the data listed in Tables 2 and 3 and the isolator configurations previously described, the values presented in Table 4 were computed. For instance, for the TFPB and DBE level, the resulting displacement is derived by adding d_2^* to d_6^*, which gives a displacement limit equal to 0.699 m. Figure 7 illustrates the adopted performance-based approach for the three examined isolator schemes. More specifically for the examined three hazard levels: dotted blue curves represent SLE, continuous red curves denote DBE, and dashed black curves correspond to MCE. A similar correlation of isolators' performance with respect to the three hazard levels has been adopted by Moeindarbari et al. [17] for TFPBs.

Table 4: PBD levels of friction pendulum isolators.

Isolator type	SLE	DBE	MCE
SFPB	-	-	0.305 m
TFPB	0.084 m	0.423 m	0.762 m
QFPB	0.095 m	0.699 m	1.04 m

Firstly, SLE level with 50% in 50 years probability of exceedance (resulting to displacement limits equal to 0.084 m for TFPBs and 0.095 m for QFPBs) is represented by the inner pendulum mechanism of the bearings; secondly, DBE level with 10% in 50 years probability of exceedance, which results to displacement limits of 0.423 m for TFPBs and 0.699 m for QFPBs; and lastly, MCE level with 2% in 50 years probability of exceedance of the maximum allowable displacement, which are equal to 0.762 m for TFPBs and 1.04 m for QFPBs. Additionally, the simple SFPB scheme is compared with the two multistage isolators, which is designed only for MCE level (with corresponding displacement limit of 0.305 m) with 2% in 50 years probability of exceedance [8].

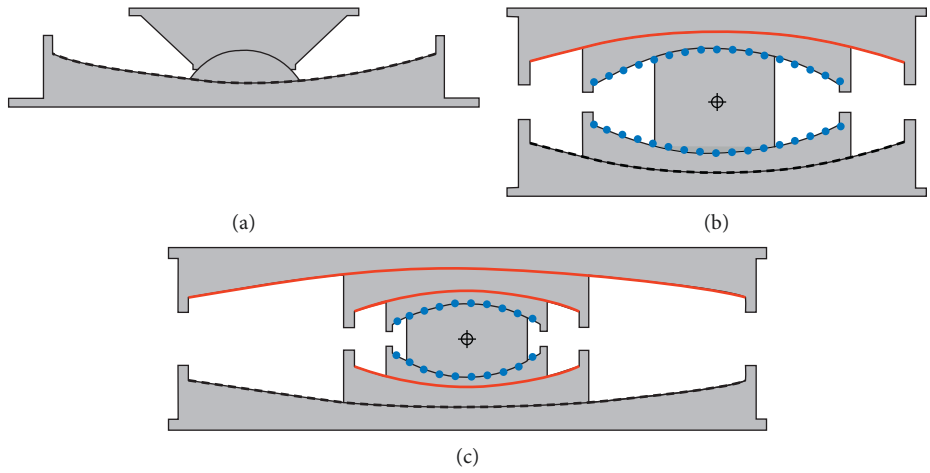

Figure 7: PBD levels in terms of isolator displacements for (a) SFPB, (b) TFPB, and (c) QFPB isolation schemes.

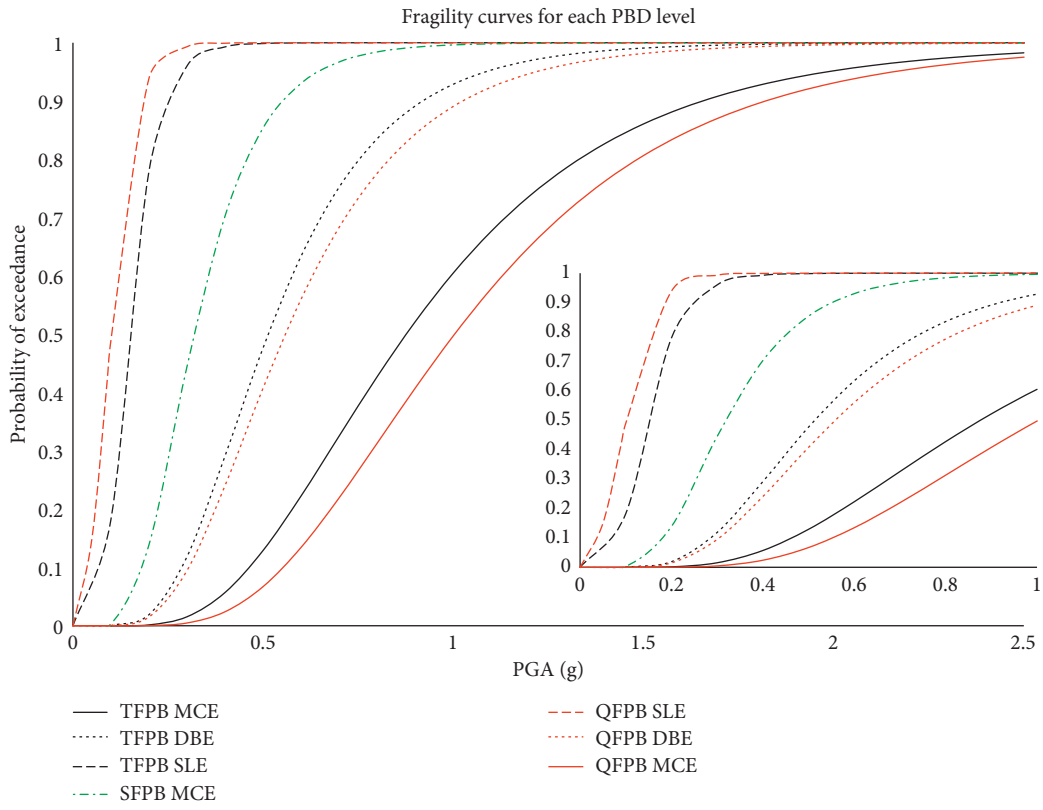

Figure 8: PBD fragility curves for SFPB, TFPB, and QFPB isolation schemes.

Accordingly, the probability of collapse considering the isolators' displacements for TFPBs and QFPBs different sliding mechanisms (depending on the hazard level) and SFPBs, is displayed in the fragility curves presented in Figure 8. Extreme PGA values are used to demonstrate the high capabilities of modern multistage isolators, while for fixed-base tanks the maximum PGA is much less (i.e., usually up to 1 g) [20, 34]. The embedded plot in Figure 8 shows the performance of all isolators within the range of more realistic expected PGA values, where the differences among the "truncated" fragility curves, especially for the lower PGA levels is more evident. It can be seen that for the case of the minor earthquake hazard scenario of SLE (where sliding occurs at the inner sliding surfaces), TFPBs presents better results than QFPBs. This is attributed to the values of friction coefficients, since TFPBs have higher values ($\mu_2 = 0.06$, $\mu_3 = 0.071$) compared to QFPB ($\mu_3 = \mu_4 = 0.01$). Thus, it is reasonable that sliding surfaces with lower values of friction coefficients will reach the displacement limit earlier than corresponding surfaces with higher values. On the other hand, for the more severe seismic scenarios of DBE and, especially, in MCE, it is evident that the QFPBs

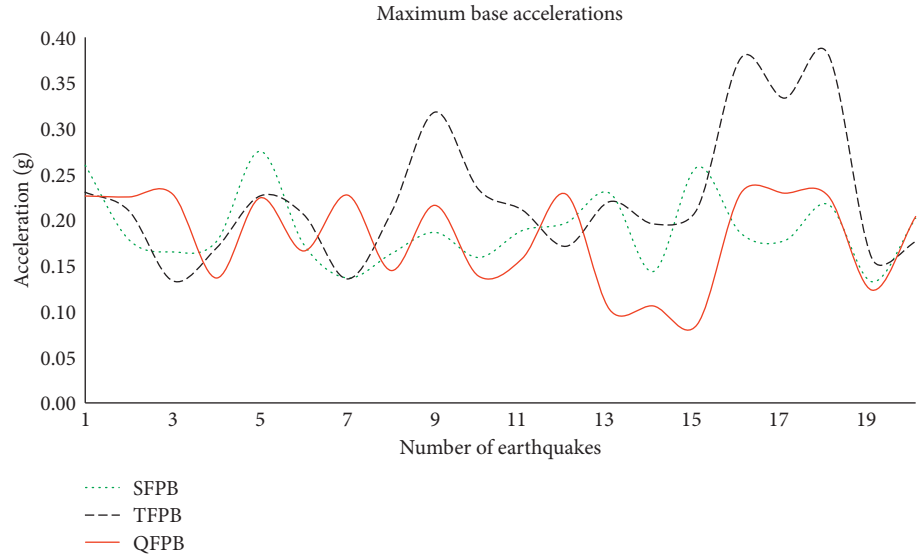

Figure 9: Base accelerations of storage tanks equipped with SFPB, TFPB, and QFPB isolators.

present significantly better results with respect to the obtained fragility estimates.

Hence, both TFPBs and QFPBs can withstand high displacement amplitudes, achieving thus lower failure probabilities even at higher seismic levels. It can be noticed that the multistage bearings of TFPBs and especially QFPBs play an important role, since they assist liquid storage tanks to maintain their structural integrity and functioning. It is also evident that these devices provide much better protection to the superstructure under severe seismic excitations compared to simple SFPBs.

6.2. Comparison of Tank Accelerations. When a fixed-base liquid storage tank is considered, then its probability of failure presents high values even for medium intensity levels (as expressed in terms of PGA values), which is not the case for base-isolated tanks [20, 34]. Base-isolation reduces the acceleration levels transmitted to the superstructure, and it can be assumed that due to isolation the tank behaves linearly even for quite high seismic intensity levels; thus, damages are avoided in the superstructure for the usually expected range of PGAs. Consequently, the emphasis related to failure of the whole system is given in the present investigation on the isolator displacements; thus, the probability of failure actually refers to the exceedance of the allowable isolators' displacement limits for various performance levels.

Nonetheless, when the imposed PGA reaches extreme values as examined herein, the transmitted acceleration, i.e., the acceleration that is measured at tank's base above the isolators, can also reach significant values, depending on the special characteristics of the excitation. This is indicatively illustrated in Figure 9, which depicts the maximum accelerations values (i.e., maximum value of the reduced acceleration transmitted to the superstructure) at the tank base level above the isolators for each of the twenty near-fault records. As it can be easily noticed, the storage tank equipped with TFPBs presents the highest values of base accelerations, especially for three records (9, 16, and 18). The superstructure isolated with SFPBs presents lower values, but as shown in the fragility analysis (Figure 8), these isolators exhibit higher collapse probabilities. In most cases, the base accelerations of storage tanks isolated with QFPBs are lower compared to those obtained by TFPBs and close to the ones corresponding to SFPBs. Therefore, it is derived that overall QFPBs present better results compared to TFPBs and SFPBs, since it is an effective isolator configuration that combines lower probabilities of collapse in terms of sliding displacements and low values of base accelerations transmitted to the superstructure.

6.3. Influence of Tank Slenderness Ratio. The plots in Figure 10 illustrate the influence of tank slenderness ratio (H/R) in the fragility curves. It is reminded that three bearing types were examined, the single-stage SFPBs and the multistage TFPBs and QFPBs. As it can be seen in this plot, due to the presence of the isolators, the fragility curves are not influenced by slenderness ratio, since there is not any significant difference among squat and slender tanks. In contrast to this finding, unanchored slender tanks are more susceptible to uplifting phenomena than the corresponding squat tanks [46]. Regarding TFPBs, for DBE and MCE levels, squat tanks are slightly less vulnerable compared to slender tanks at low to medium PGA values. For increased seismic intensity and higher probability of collapse, the fragility curves are almost identical. For SLE level, there is not any observable difference. In the case of SFPBs and for MCE scenario, squat tanks are slightly less vulnerable than slender tanks for PGA values between 0.5 g and 1.0 g. For the case of QFPBs, SLE and DBE levels do not present any difference, while for the MCE level, the slender tanks are marginally less vulnerable compared to squat tanks at low PGA values.

6.4. Influence of λ_{max} Factor. A fragility analysis considering performance deterioration due to aging, contamination, etc.

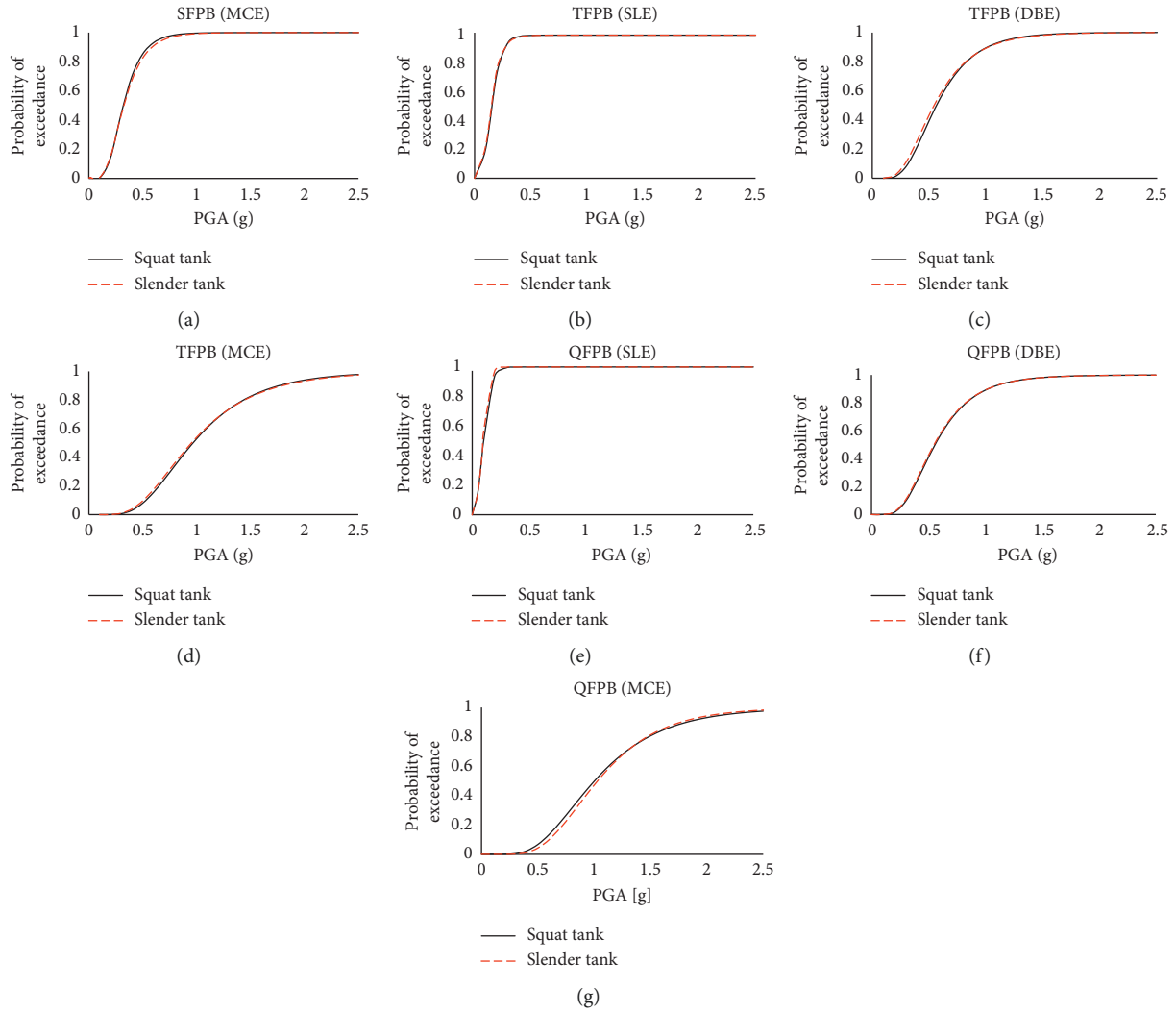

Figure 10: PBD fragility curves of squat and slender tanks using SFPBs, TFPBs, and QFPBs isolators.

of isolators is performed for the squat tank, by incorporating λ_{max} factor in the design of TFPBs friction isolators. This parameter is directly applied to the nominal value of the coefficient of friction to forecast aging and deterioration phenomena that will affect the performance of friction isolation bearings [47]. According to the recommendations of Constantinou et al. [27], the value of 1.1 is selected for aging and 1.05 for contamination, and λ_{max} factor is calculated as the product of these two values.

As it can be noticed from Figure 11, the incorporation of λ_{max} in the design of friction isolators for the squat tank affects the results for the more severe hazard levels. Especially for the higher seismicity intensity levels (DBE), the TFPBs designed with the factor λ_{max} present better performance, while for the low seismicity intensity level (SLE), there are only marginal differences.

7. Conclusions

2In this paper, the seismic vulnerability of liquid storage tanks isolated with three types of sliding bearings, namely, SFPBs and the multistage TFPBs and QFPBs were investigated. More specifically, the displacement capacity of SFPBs and of the different pendulum mechanisms of TFPBs and QFPBs were associated to three PBD levels (SLE, DBE, and MCE) by performing repeated dynamic nonlinear analyses. A high displacement capacity is a very crucial parameter for the isolators used to protect such critical infrastructures, especially against severe near-fault earthquakes. Additionally, the resulting base accelerations transmitted at the storage tanks isolated with the aforementioned devices were compared. In order to achieve optimal balance between computational efficiency and accuracy, simplified models were developed for the realistic representation of the hydrodynamic response of liquid storage tanks.

The following conclusions can be derived from the present investigation:

(a) Friction isolation bearings with multistage and adaptive behavior (TFPBs and mostly QFPBs) present superior seismic performance compared to

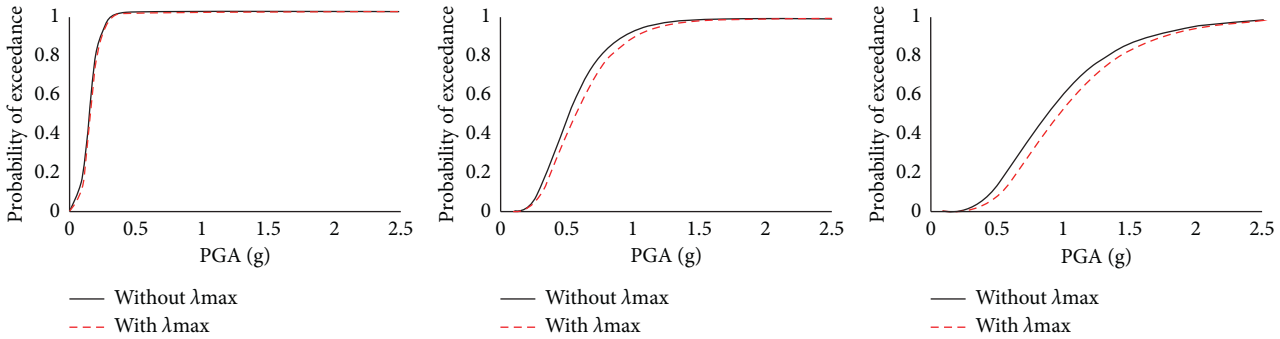

Figure 11: Comparison of λ_{max} factor influence on TFPBs friction bearings' performance for the squat tank. (a) SLE. (b) DBE. (c) MCE.

single bearings (SFPBs). Thus, they have the ability of accommodating much larger displacements (i.e., higher PGA demand levels).

(b) In general, as expected, the QFPB is the superior isolator device due to its ability to withstand higher displacements at different PBD levels.

(c) Regarding the base accelerations of storage tanks isolated with different friction bearings, the best results are derived from the superstructure equipped with QFPBs. A QFPB is an efficient base-isolation scheme that can combine the accommodation of large displacement amplitudes of near-fault excitations with low base acceleration values. Thus, it can protect the structural integrity of such critical infrastructure even at high seismic demand levels.

(d) The slenderness ratio of the cylindrical base-isolated storage tanks via SFPBs, TFPBs, and QFPBs do not significantly affect the fragility estimations when maximum isolator displacements are considered.

(e) The future performance deterioration in the design of sliding bearings, represented by the factor λ_{max}, can influence the fragility analysis results. More specifically, when this factor is incorporated in the analysis, the base-isolated liquid storage tanks present a slightly less vulnerable performance for the higher seismic demand levels.

Abbreviations

3D: Three-dimensional
CDF: Cumulative Distribution Function
CSB: Concave Sliding Bearing
DBE: Design Basis Earthquake
DI: Damage Index
DVFPS: Double Variable Frequency Pendulum System
EDP: Engineering Demand Parameter
ELF: Equivalent Linear Force
EPS: Earthquake Protection Systems
FNA: Fast Nonlinear Analysis
FP: Friction Pendulum
HDRB: High Damping Rubber Bearing
IDA: Incremental Dynamic Analysis
IM: Intensity Measure
LNG: Liquefied Natural Gas
MCE: Maximum Credible Earthquake
MFPS: Multiple Friction Pendulum System
MSDA: Multistripe Dynamic Analysis
NATECH: Natural and Technological disasters
PBD: Performance-Based Design
PGA: Peak Ground Acceleration
QFPB: Quintuple Friction Pendulum System
SFPB: Single Friction Pendulum Bearing
SLE: Service Level Earthquake
TFPB: Triple Friction Pendulum Bearing
VCFPS: Variable Curvature Friction Pendulum System
VFPS: Variable Friction Pendulum System.

Data Availability

The data supporting the results reported in the article are quite huge. Nevertheless, interested readers may access these data of the study by directly asking authors to provide them.

Disclosure

An earlier version of this work was presented as a poster at the Second Young Researchers Workshop of Hellenic Society of Earthquake Engineering, 3/11/2017, Athens, Greece.

Conflicts of Interest

The authors declare that there are no conflicts of interest regarding the publication of this paper.

Acknowledgments

This research has been generously supported by Bakopouleio Foundation, Greece, via a Ph.D. scholarship for the first author, which is gratefully acknowledged. The authors would also like to thank Mr. Donghun Lee for providing useful insight regarding the QFPB analytical model.

References

[1] G. Housner, "The dynamic behavior of water tanks," *Bulleting of the Seismological Society of America*, vol. 53, no. 2, pp. 381–387, 1963.

[2] T. Larkin, "Seismic response of liquid storage tanks incorporating soil structure interaction," *ASCE Journal of*

Geotechnical and Geoenvironmental Engineering, vol. 134, no. 12, pp. 1804–1814, 2008.

[3] P. K. Malhotra, "Seismic response of soil-supported unanchored-liquid storage tanks," *ASCE Journal of Structural Engineering*, vol. 123, no. 4, pp. 440–450, 1997.

[4] A. S. Veletsos, Y. Tang, and H. T. Tang, "Dynamic response of flexibly supported liquid-storage tanks," *ASCE Journal of Structural Engineering*, vol. 118, no. 1, pp. 264–289, 1992.

[5] K. Bakalis, D. Vamvatsikos, and M. Fragiadakis, "Seismic risk assessment of liquid storage tanks via a nonlinear surrogate model," *Earthquake Engineering and Structural Dynamics*, vol. 46, no. 15, pp. 2851–2868, 2017.

[6] T. Kelly, *Base Isolation of Structures-Design Guidelines*, Holmes Consulting Group Ltd., Auckland, New Zealand, 2001.

[7] M. R. Shekari, N. Khaji, and M. T. Ahmadi, "On the seismic behavior of cylindrical base-isolated liquid storage tanks excited by long-period ground motions," *Soil Dynamics and Earthquake Engineering*, vol. 30, no. 10, pp. 968–980, 2010.

[8] EPS, *Earthquake Protection Systems*, 2011, http://www.earthquakeprotection.com.

[9] V. R. Panchal and D. P. Soni, "Seismic behavior of isolated fluid storage tanks: a-state-of-the-art review," *KSCE Journal of Civil Engineering*, vol. 18, no. 4, pp. 1097–1104, 2014.

[10] Y. P. Wang, M. C. Teng, and K. W. Chung, "Seismic isolation of rigid cylindrical tanks using friction pendulum bearings," *Earthquake Engineering and Structural Dynamics*, vol. 30, no. 7, pp. 1083–1099, 2001.

[11] M. B. Jadhav and R. S. Jangid, "Response of base-isolated liquid storage tanks," *Shock and Vibration*, vol. 11, no. 1, pp. 33–45, 2004.

[12] V. R. Panchal and R. S. Jangid, "Variable friction pendulum system for seismic isolation of liquid storage tanks," *Nuclear Engineering and Design*, vol. 238, no. 6, pp. 1304–1315, 2008.

[13] E. Abali and E. Uckan, "Parametric analysis of liquid storage tanks base isolated by curved surface sliding bearings," *Soil Dynamics and Earthquake Engineering*, vol. 30, pp. 21–31, 2010.

[14] D. P. Soni, P. P. Mistry, R. S. Jangid, and V. R. Panchal, "Seismic response of the double variable frequency pendulum isolator," *Structural Control and Health Monitoring*, vol. 18, no. 4, pp. 450–470, 2011.

[15] A. A. Seleemah and M. El-Sharkawy, "Seismic analysis and modeling of isolated elevated liquid storage tanks," *Earthquakes and Structures*, vol. 2, no. 4, pp. 397–412, 2011.

[16] V. R. Panchal and R. S. Jangid, "Behaviour of liquid storage tanks with VCFPS under near-fault ground motions," *Structure and Infrastructure Engineering*, vol. 8, no. 1, pp. 71–88, 2012.

[17] H. Moeindarbari, M. Malekzadeh, and T. Taghkikhany, "Probabilistic analysis of seismically isolated elevated liquid storage tank using multi-phase friction bearing," *Earthquakes and Structures*, vol. 6, no. 1, pp. 111–125, 2014.

[18] F. Paolacci, "On the effectiveness of two isolation systems for the seismic protection of elevated tanks," *Journal of Pressure Vessels Technology*, vol. 137, no. 3, article 031801, 2015.

[19] S. Bagheri and M. Farajian, "The effects of input earthquake characteristics on the nonlinear dynamic behavior of FPS isolated liquid storage tanks," *Journal of Vibration and Control*, vol. 24, no. 7, pp. 1264–1282, 2016.

[20] H. N. Phan, F. Paolacci, D. Corritore, B. Akbas, E. Uckan, and J. J. Shen, "Seismic vulnerability mitigation of liquefied gas tanks using concave sliding bearings," *Bulleting of Earthquake Engineering*, vol. 14, no. 11, pp. 3283–3299, 2016.

[21] D. Lee and M. C. Constantinou, "Quintuple friction pendulum isolator: behavior, modeling and validation," *Earthquake Spectra*, vol. 32, no. 3, pp. 1607–1626, 2016.

[22] A. Tsipianitis and Y. Tsompanakis, "Seismic vulnerability assessment of base-isolated liquid fuels tanks," in *Proceedings of 12th International Conference on Structural Safety and Reliability (ICOSSAR)*, Vienna, Austria, August 2017.

[23] K. Bakalis, M. Fragiadakis, and D. Vamvatsikos, "Surrogate modeling for the seismic performance assessment of liquid storage tanks," *Journal of Structural Engineering*, vol. 143, no. 4, article 04016199, 2016.

[24] V. A. Zayas, S. S. Low, and S. A. Mahin, "The FPS earthquake resisting system-experimental report," Report No. UCB/EERC-8701, Earthquake Engineering Research Center, College of Engineering, University of California, Berkeley, CA, USA, 1987.

[25] D. M. Fenz and M. C. Constantinou, "Spherical sliding isolation bearings with adaptive behavior: theory," *Earthquake Engineering and Structural Dynamics*, vol. 37, no. 2, pp. 163–183, 2008.

[26] T. A. Morgan, *The use of innovative base isolation systems to achieve complex seismic performance objectives*, Ph.D. Dissertation, Department of Civil and Environmental Engineering, University of California, Berkeley, CA, USA, 2007.

[27] M. C. Constantinou, I. Kalpakidis, A. Filiatrault, and R. A. E. Lay, "LRFD-based analysis and design procedures for bridge bearings and seismic isolators," Report No. MCEER-11-0004, Multidisciplinary Center for Earthquake Engineering Research, University of Buffalo, New York, NY, USA, 2011.

[28] N. D. Dao, K. L. Ryan, E. Sato, and T. Sasaki, "Predicting the displacement of triple pendulum bearing in a full-scale shaking experiment using a three-dimensional element," *Earthquake Engineering and Structural Dynamics*, vol. 42, no. 11, pp. 1677–1695, 2013.

[29] CSI, *SAP 2000 Version 18, Integrated Software for Structural Analysis and Design, Analysis Reference Manual*, Computer & Structures Inc., Berkeley, CA, USA, 2016.

[30] A. Kasalanati and M. C. Constantinou, "Experimental study of bridge elastomeric and other isolation and energy dissipation systems with emphasis on uplift prevention and high velocity near source seismic excitation," Technical Report, MCEER-99-0004, Multidisciplinary Center for Earthquake Engineering Research, University at Buffalo, Buffalo, NY, USA, 1999.

[31] D. Vamvatsikos and C. A. Cornell, "Incremental dynamic analysis," *Earthquake Engineering and Structural Dynamics*, vol. 31, no. 3, pp. 491–514, 2002.

[32] J. W. Baker, "Efficient analytical fragility function fitting using dynamic structural analysis," *Earthquake Spectra*, vol. 31, no. 1, pp. 579–599, 2015.

[33] K. Bakalis, D. Vamvatsikos, and M. Fragiadakis, "Seismic fragility assessment of steel liquid storage tanks," in *Proceedings of the ASME 2015 Pressure Vessels and Piping Conference*, Boston, Massachusetts, USA, 2015.

[34] S. K. Saha, V. A. Matsagar, and A. K. Jain, "Seismic fragility of base-isolated water storage tanks under non-stationary earthquakes," *Bulletin of Earthquake Engineering*, vol. 14, no. 4, pp. 1153–1175, 2016.

[35] M. A. Haroun, "Vibration studies and tests of liquid storage tanks," *Earthquake Engineering and Structural Dynamics*, vol. 11, no. 2, pp. 179–206, 1983.

[36] S. Kilic and Z. Ozdemir, "Simulation of sloshing effects in cylindrical containers under seismic loading," in *Proceedings*

of the 6th LS-DYNA Anwenderforum DYNAmore, Dresden, Germany, 2007.

[37] A. Di Carluccio and G. Fabbrocino, "Some remarks on the seismic demand estimation in the context of vulnerability assessment of large steel storage tank facilities," *ISRN Civil Engineering*, vol. 2012, Article ID 271414, 12 pages, 2012.

[38] CEN, *Eurocode 8: Design of structures for earthquake resistance-Part 4: Silos, Tanks and Pipelines*, European Committee for Standardization, Brussels, Belgium, 2006.

[39] I. P. Christovasilis and A. S. Whittaker, "Seismic analysis of conventional and isolated LNG tanks using mechanical analogs," *Earthquake Spectra*, vol. 24, no. 3, pp. 599–616, 2008.

[40] R. A. Ibrahim, "Recent advances in nonlinear passive vibration isolators," *Journal of Sound and Vibration*, vol. 314, no. 3–5, pp. 371–452, 2008.

[41] Y. Bouassida, E. Bouchon, P. Crespo et al., *Bridge Design to Eurocodes-Worked Examples*, JRC Scientific and Technical Reports , EUR 25193 EN-2012, 2012.

[42] P. Sommerville, N. Smith, S. Punyamurthula, and J. Sun, "Development of ground motion time histories for phase 2 of the FEMA/SAC Steel Project," NISEE Report: SAC/BD-97-04, SAC Joint Venture, Sacramento, CA, USA, 1997.

[43] A. H. M. M. Billah and M. S. Alam, "Seismic fragility assessment of concrete bridge pier reinforced with superelastic shape memory alloy," *Earthquake Spectra*, vol. 31, no. 3, pp. 1515–1541, 2015.

[44] M. A. Haroun and G. W. Housner, "Seismic design of liquid storage tanks," *Journal of the Technical Councils of ASCE*, vol. 107, pp. 191–207, 1981.

[45] P. K. Malhotra, T. Wenk, and M. Wieland, "Simple procedure for seismic analysis of liquid-storage tanks," *Structural Engineering International*, vol. 10, no. 3, pp. 197–201, 2000.

[46] P. K. Malhotra and A. S. Veletsos, "Uplifting response of unanchored liquid-storage tanks," *ASCE Journal of Structural Engineering*, vol. 120, no. 12, pp. 3525–3547, 1994.

[47] M. C. Constantinou, A. S. Whittaker, Y. Kalpakidis, D. M. Fenz, and G. P. Warn, *Performance of seismic isolation hardware under service and seismic loading*, Report No. MCEER-07-0012, Multidisciplinary Center for Earthquake Engineering Research, University of Buffalo, New York, NY, USA, 2007.